PHOTOSYNTHETICA
International Journal for Photosynthesis Research

DOI 10.32615/ps.2026.006 PHOTOSYNTHETICA 64 (2): 73-81, 2026

Exploring prediction mechanisms for temperature-induced variation in maximum carboxylation rate from spectral reflectance across 450–850 nm in cucumber leaves

T. SHIBATA[*], H. YAMAGUCHI[*], S. KUBOTA[**], D. YASUTAKE[**,***], T. HIROTA[**], and G. YOKOYAMA[**,+]

Graduate School of Bioresource and Bioenvironmental Sciences, Kyushu University, 744 Motooka, Nishi-ku, 819-0395 Fukuoka, Japan[*]
Faculty of Agriculture, Kyushu University, 744 Motooka, Nishi-ku, 819-0395 Fukuoka, Japan[**]
IoP Collaborative Creation Center, Kochi University, 200 Otsu, Monobe, Kochi, 783-8502 Nankoku City, Japan[***]

Abstract

Leaf spectral reflectance across 450–850 nm has been shown to predict maximum carboxylation rate (V_{cmax}), which varies with leaf temperature (T_{leaf}). However, the mechanism by which temperature-induced variation in V_{cmax} is predicted from reflectance remains unclear. The objective of this study was to explore this mechanism using spectral reflectance across 450–850 nm. We measured V_{cmax} across a range of T_{leaf} (18–31°C) and reflectance in cucumber (*Cucumis sativus* L.) leaves. Partial least squares regression models moderately predicted V_{cmax} (R^2 = 0.73), whereas T_{leaf} was weakly predicted (R^2 = 0.32). When only visible reflectance (450–700 nm) was used, prediction accuracy for both V_{cmax} and T_{leaf} declined (R^2 = 0.59 and 0.17). Because predicting T_{leaf} from reflectance suggests that temperature-related information may help predict temperature-induced variations in V_{cmax}, our results indicate that reflectance in 700–850 nm possibly captures temperature-induced variation in V_{cmax}.

Keywords: *Cucumis sativus* L.; leaf temperature; maximum carboxylation rate; partial least squares regression; photosynthesis; reflectance spectroscopy.

Highlights

- Maximum carboxylation rate was predicted *via* leaf spectral reflectance in 450–850 nm
- Leaf temperature was only partially captured by the reflectance in 450–850 nm
- Reflectance in 700–850 nm may detect temperature shifts in the maximum carboxylation rate

Received 17 December 2025
Accepted 1 April 2026
Published online 13 April 2026

[+]Corresponding author
e-mail: gaku.yokoyama.728@m.kyushu-u.ac.jp

Abbreviations: BIAS – difference between the mean predicted values and the mean observed values divided by the mean observed values; C_i – intercellular CO_2 concentration; E_a – activation energy; E_a (K_c) – activation energy for Michaelis–Menten constant for CO_2; E_a (K_o) – activation energy for Michaelis–Menten constant for O_2; E_a (Γ*) – activation energy for CO_2-compensation point in the absence of mitochondrial respiration at 25°C; k_{25} (K_c) – Michaelis–Menten constant for CO_2 at 25°C; k_{25} (K_o) – Michaelis–Menten constant for O_2 at 25°C; k_{25} (Γ*) – Michaelis–Menten constant for CO_2-compensation point in the absence of mitochondrial respiration at 25°C; K_c – Michaelis–Menten constant for CO_2; K_m – Michaelis–Menten constant; K_o – Michaelis–Menten constant for O_2; MBE – mean bias error; NIR – near-infrared; O_i – intercellular O_2 concentration; PLSR – partial least squares regression; P_{Nmax} – light-saturated net photosynthetic rate; R – universal gas constant; R^2 – coefficient of determination; R_d – mitochondrial respiration rate in the light; RMSE – root mean square error; RMSEP – root mean square error of prediction; RuBP – ribulose-1,5-bisphosphate; SWIR – short-wave infrared; T_{leaf} – leaf temperature; V_{cmax} – maximum carboxylation rate; V_{cmax25} – maximum carboxylation rate normalized to 25°C; VIP – variable importance in projection; VIS – visible; VPD – vapor pressure deficit; Γ* – CO_2-compensation point in the absence of mitochondrial respiration; %RMSEP – root mean square error of prediction as a percentage of the trait range.

Acknowledgments: This work was supported by the Kyushu University Reform and Revitalization System, Grants-in-Aid for Scientific Research (JSPS KAKENHI Grant Number JP21H02318, JP23K14046, and JP25H00953), and Cabinet Office grants in aid 'The Advanced Next-Generation Greenhouse Horticulture by IoP (Internet of Plants)' and 'Evolution to Society 5.0 Agriculture Driven by IoP (Internet of Plants)', Japan.

Conflict of interest: The authors declare that they have no conflict of interest.

Introduction

Leaf spectroscopy has received increasing attention as a promising tool for predicting the photosynthetic capacity of leaves, namely maximum carboxylation rate, V_{cmax}, or the values of this rate normalized to a given leaf temperature, which is typically 25°C, V_{cmax25} (Farquhar *et al*. 1980, Serbin *et al*. 2012, Fu *et al*. 2020, Meacham-Hensold *et al*. 2020, Buchaillot *et al*. 2022, Kumagai *et al*. 2022). The prediction of leaf traits (*e.g.*, V_{cmax}) using spectroscopy is based on the principle that the spectral distribution of leaves, generally in the wavelength range of 400–2,500 nm, reflects the spectral absorption characteristics and the quantity of chemical substances (*e.g.*, chlorophyll, water, and nitrogen) contained in the leaves, as well as the leaf structure (Knipling 1970). Because leaf photosynthetic capacity is closely related to leaf nitrogen and chlorophyll content, this relationship likely explains why spectroscopy is effective for estimating the content of photosynthetic proteins (*e.g.*, Rubisco), that is the photosynthetic capacity normalized to a standard temperature such as 25°C (*i.e.*, V_{cmax25}) (Kattge *et al*. 2009, Croft *et al*. 2017). In fact, some studies have reported that the correlation of leaf spectral distribution with chlorophyll and nitrogen content is the primary mechanism underlying the prediction of V_{cmax25} using partial least squares regression, PLSR – a statistical technique commonly employed to predict leaf traits from spectral reflectance by reducing multicollinearity among wavelengths (Wold *et al*. 2001, Dechant *et al*. 2017, Yendrek *et al*. 2017, Kumagai *et al*. 2022).

Interestingly, several studies have reported that V_{cmax}, which varies in response to short-term (*i.e.*, seconds to hours) fluctuations in leaf temperature, can be predicted using spectral reflectance (Serbin *et al*. 2012, Fu *et al*. 2020, Meacham-Hensold *et al*. 2020, Buchaillot *et al*. 2022). These temperature-induced changes in V_{cmax} are attributed to the temperature-dependent activity of photosynthetic proteins (*e.g.*, Rubisco), rather than to the amount of chlorophyll or nitrogen in leaves (Bernacchi *et al*. 2001, Hikosaka *et al*. 2006, Bernacchi *et al*. 2013). Therefore, spectral reflectance appears to capture information that correlates with variations in V_{cmax} caused by short-term fluctuations in leaf temperature; however, the theoretical basis for the relationship between leaf spectral reflectance and temperature-related variations in V_{cmax} remains unclear.

Despite the growing number of studies that targeting prediction of V_{cmax} using spectroscopy, very few have investigated the underlying reasons why such prediction is possible (Khan *et al*. 2021). Khan *et al*. (2021) reported that leaf temperature could be predicted using a multiple regression model based on reflectance at 697; 1,400; 1,507; and 1,531 nm, indicating that the spectral region related to leaf temperature lies largely in the short-wave infrared region (SWIR; 1,000–2,500 nm), although the visible and near-infrared region (VIS and NIR; 400–1,000 nm) may also contain temperature-related signals. The ability to predict leaf temperature from spectral reflectance suggests that information related to leaf temperature may be used to predict temperature-induced variations in V_{cmax}. In fact, several studies have reported that variations in V_{cmax} due to changes in leaf temperature can be predicted from reflectance within 450–850 nm (Silva-Perez *et al*. 2018, Fu *et al*. 2020, Meacham-Hensold *et al*. 2020, Buchaillot *et al*. 2022), and even within the VIS region (450–700 nm; Sexton *et al*. 2021). These studies supported that reflectance associated with leaf temperature may exist within these wavelengths; however, the underlying mechanisms have not been examined.

As a first step toward exploring the mechanisms underlying the prediction of V_{cmax} and its temperature-induced variation from leaf spectral reflectance in 450–850 nm, we aimed to evaluate (*1*) whether leaf spectral reflectance in this range can predict V_{cmax}, leaf temperature, and V_{cmax25}, and (*2*) how much leaf temperature or V_{cmax25} affects the prediction of V_{cmax}. To achieve these aims, we measured V_{cmax}, leaf temperature, V_{cmax25}, and spectral reflectance within 450–850 nm because of spectrometer noise, across a range of leaf temperatures (18 to 31°C) in cucumber (*Cucumis sativus* L., cv. Natsu Suzumi). We then constructed PLSR models to predict V_{cmax}, leaf temperature, and V_{cmax25} from spectral reflectance in 450–850 nm. To identify the wavelengths most important for predicting V_{cmax}, leaf temperature, and V_{cmax25}, we analyzed the regression coefficients and variable importance in projection, VIP scores of the constructed PLSR models. Finally, we calculated the score and loading values of the first and second components in the prediction of V_{cmax} and compared their relationships with leaf temperature and V_{cmax25}.

Materials and methods

Plant materials and growth conditions: Cucumbers (*Cucumis sativus* L., cv. Natsu Suzumi) were cultivated in a greenhouse located at the Ito Plant Experiment Fields & Facilities, Faculty of Agriculture, Kyushu University, Fukuoka, Japan (33°35.5'N, 130°12.9'E). Three seeds were sown per 0.35-L pot filled with vermiculite; 60 pots were prepared on 19 June 2022, and 12 pots were prepared on 5 August 2022. The plants were irrigated with tap water for up to two weeks after sowing. Afterwards, the plants were thinned to two plants per pot, and the removed plants were not used in the experiments. After two weeks following sowing, the plants were treated with liquid fertilizers (*OAT House 1*, and *OAT House 2*, *OAT Agrio Co.*, *Ltd*., Tokyo, Japan) with different electrical conductivities (electrical conductivity = 0.5, 1.0, 1.5, 2.0, and 2.5 mS cm^{-1}) to create variations in the photosynthetic capacity of the leaves and prevent overfitting.

Measurement and estimation of leaf photosynthetic capacity: The following experiments were conducted in a plant growth chamber (*HNM-S11*, *Koito Electric Industries*, *Ltd*., Shizuoka, Japan; growth area: length: 60.0 cm × width: 90.0 cm × height: 90.0 cm) at a laboratory in Kyushu University on: 19, 21, 22, 30, and 31 July 2022; 1, 2, and 3 August 2022; 4 and 10 September 2022. A total of 59 leaves (one leaf per plant), corresponding to the third or fourth fully expanded leaves, were sampled

for the experiments. Leaf gas exchange was measured using a portable gas-exchange measurement system (*LI-6400XT*, *Li-COR Inc*., Lincoln, NE, USA). The light-saturated net photosynthetic rate (P_{Nmax}; μmol m^{-2} s^{-1}) and the intercellular CO_2 concentration (C_i; μmol mol^{-1}) at the ambient CO_2 concentrations of 300 μmol mol^{-1} were measured under a PPFD of 1,500 μmol m^{-2} s^{-1}, which is enough to expose leaves to saturated light, and a vapor pressure deficit (VPD) of 1–2 kPa. During gas-exchange measurements, the *LI-6400XT*'s temperature-controlled cuvette was set to target leaf temperatures (*e.g*., 20, 25, and 30°C), while the air temperature inside the growth chamber was also adjusted to match these settings within a range of 18–31°C and relative humidity inside the growth chamber was set to 70% following Nakai *et al*. (2023).

V_{cmax} [μmol m^{-2} s^{-1}] was calculated using P_{Nmax} and C_i at ambient CO_2 concentrations of 300 μmol mol^{-1}, using the one-point method as described by Wilson *et al*. (2000), De Kauwe *et al*. (2016), and Burnett *et al*. (2019). V_{cmax} was calculated, assuming that leaf photosynthesis is limited by ribulose-1,5-bisphosphate (RuBP) under saturated-light conditions and CO_2 concentrations of 300 μmol mol^{-1} and that mitochondrial respiration rate in the light (R_d) is 1.5% of V_{cmax}, as follows:

$$V_{cmax} = \frac{P_{Nmax}}{\frac{C_i - \Gamma^*}{C_i + K_m} - 0.015} \quad (1)$$

where K_m is the Michaelis–Menten constant [μmol mol^{-1}], and Γ* is the CO_2-compensation point in the absence of mitochondrial respiration [μmol mol^{-1}]. Herein, K_m is described as follows:

$$K_m = K_c\left(1 + \frac{O_i}{K_o}\right) \quad (2)$$

where K_c is the Michaelis–Menten constant for CO_2 [μmol mol^{-1}], K_o is the Michaelis–Menten constant for O_2 [mmol mol^{-1}], and O_i is the intercellular O_2 concentration assumed to be 210 mmol mol^{-1}. The temperature dependence of Γ*, K_c, K_o, and V_{cmax} was described using the Arrhenius function:

$$\text{Parameter}_{T_{leaf}} = \text{Parameter}_{25} \times \exp\left[\frac{E_a(T_{leaf} + 273.15) - 298.15}{298.15R(T_{leaf} + 273.15)}\right] \quad (3)$$

where T_{leaf} is the leaf temperature [°C], Parameter_{25} is the parameter value at 25°C, E_a is the activation energy [J mol^{-1}], and R is the universal gas constant (8.31 J K^{-1} mol^{-1}).

Because 72 out of 247 V_{cmax} values were incorrectly calculated due to an erroneous Eq. 1 described in De Kauwe *et al*. (2016), these data were corrected using a regression line based on the relationship between the correct and incorrect values of V_{cmax}, as shown in Fig. 1S (*supplement*). All parameter values referenced from other papers for calculating V_{cmax} were summarized in Table 1S (*supplement*).

Additionally, the estimation accuracy of the one-point method was tested by comparing the estimated V_{cmax} values with those obtained from the CO_2 response (P–C_i) curve method following Kubota *et al*. (2026). To estimate V_{cmax} from the P–C_i curve method, the '*Plantecophys*' package in *R* (Duursma 2015) was used. The one-point method showed a high coefficient of determination (R^2 = 0.74), a small estimation bias (MBE = –0.41 μmol m^{-2} s^{-1}), and a small root mean square error (RMSE = 5.72 μmol m^{-2} s^{-1}) (Fig. 2S, *supplement*), suggesting that the difference in the V_{cmax} estimation method does not affect the results of this study.

Measurements of leaf spectral reflectance and postprocessing: The spectral reflectance of each leaf was measured immediately after the gas-exchange measurement of the same leaf. Since ambient temperature was maintained at the target values (*e.g*., 20, 25, and 30°C) using a growth chamber and leaf temperature had been controlled by the temperature-regulated cuvette of the *LI-6400XT* immediately before the reflectance measurements, we assumed that leaf temperature remained stable during the reflectance measurements. Leaf spectral reflectance was collected using the measurement system shown in Fig. 1. The measurement system consisted of an LED light source (*BBSMD3535-BB1-60-010*, *Phoenix Electric Co.*, *Ltd*., Hyogo, Japan), a light-condensing pipe (height: 5 cm), and a spectrometer (*BIM-6002A-10-S03L00F06G02*, *Yixi Intelligent Technology*, Hangzhou, China) attached to an optical fiber probe (*SIM-6102-0615*, *Yixi Intelligent Technology*, Hangzhou, China). The spectral output of the LED light source in the range of 400–900 nm did not mimic solar radiation (Fig. 3S, *supplement*). The light-condensing pipe was made by a 3D-printer (*Da Vinci Jr. Pro X+ 3FJSPXJP00G*, *XYZprinting Inc*., Taiwan) and its inner walls were coated with barium sulfate (*Pre-Mix White Reflectance Coating*, *Edmund Optics Inc*., AZ, USA) to scatter light in the condensing pipe. The size and aperture area of the light-condensing pipe were shown in Fig. 3S. The elevation angle of the optical fiber probe was 45°, and the vertical distance to the leaf surface was 5 mm (Fig. 4S, *supplement*). The spectral resolution of the spectrometer was 1 nm, and its measurable wavelength range was 300–1,000 nm. Before each measurement, reference spectra were measured using a standard white panel (*0605221 IQ white reference*, *Specim Spectral Imaging Ltd*., Oulu, Finland), requiring approximately 30 seconds. The leaf spectral reflectance was measured five times per leaf, avoiding the midrib, taking approximately 30 seconds in total. The measured spectral reflectance of each leaf was averaged, and the averaged reflectance was smoothed by spline interpolation. Due to the significant noise at the edges of the measurable wavelength range of the spectrometer, the leaf hyperspectral reflectance in the ranges of 300–450 nm and 850–1,000 nm was excluded, and thus, spectral reflectance from 450–850 nm was used for analysis. At the same time as the leaf reflectance measurement, the leaf temperature was measured using a T-type thermocouple (diameter: 0.2 mm).

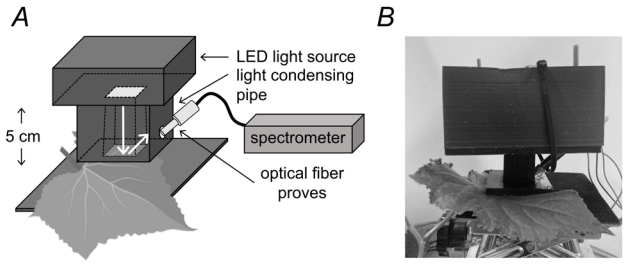

Fig. 1. Schematic of the measurement system for leaf spectral reflectance (*A*) and photograph of the system (*B*).

Statistical analysis of leaf spectral reflectance data: To obtain V_{cmax} at leaf temperatures during leaf reflectance measurements, we subsequently calculated V_{cmax} at the leaf temperatures recorded during the spectral measurements using the temperature dependence of V_{cmax} estimated from Eq. 3, although leaf temperature during the spectral reflectance measurements was almost identical to that during the gas-exchange measurements.

V_{cmax}, leaf temperature, and V_{cmax25} were predicted from the leaf spectral reflectance in 450–850 nm (including the NIR region) using respective PLSR models. In addition, to clarify whether the spectral reflectance within the VIS region can detect V_{cmax}, leaf temperature, and V_{cmax25}, these leaf traits were identically predicted from the spectral reflectance in 450–700 nm. Before inputting the measured V_{cmax}, leaf temperature, and V_{cmax25} values into the PLSR models, we performed the Shapiro–Wilk test and a skewness test for each variable because objective variables in PLSR models are ideally normally distributed and not significantly skewed (Sawatsky *et al*. 2015, Burnett *et al*. 2021). As a result of these statistical tests, data of V_{cmax} and leaf temperature were not distributed normally and V_{cmax25} was distributed normally, while V_{cmax} was skewed to the right and leaf temperature and V_{cmax25} were not significantly skewed (Fig. 2). We then constructed PLSR models using square root transformed data of V_{cmax}, leaf temperature, and V_{cmax25}. However, the variation patterns of the regression coefficients and VIP values were largely consistent with those obtained from the PLSR models constructed using untransformed data for all predictions (V_{cmax}, leaf temperature, and V_{cmax25}), and the prediction accuracies for leaf temperature and V_{cmax25} were not improved when the transformed data were used. Thus, we used the original data for the prediction of leaf temperature and V_{cmax25}, and the square root transformed data for the prediction of V_{cmax}.

We constructed respective PLSR models for each objective variable (*i.e.*, V_{cmax} and leaf temperature: n = 247; V_{cmax25}: n = 59) largely following the approach of Burnett *et al*. (2021). First, each dataset including explanatory variables (leaf spectral reflectance from 450–850 nm or 450–700 nm) and objective variables (V_{cmax}, leaf temperature, or V_{cmax25}) was randomly divided into a calibration dataset (70%) and a validation dataset (30%). Especially, for the prediction of V_{cmax25}, leaf spectral reflectance from 450–850 nm at leaf temperature of 25°C was used as explanatory variable. Second, the calibration

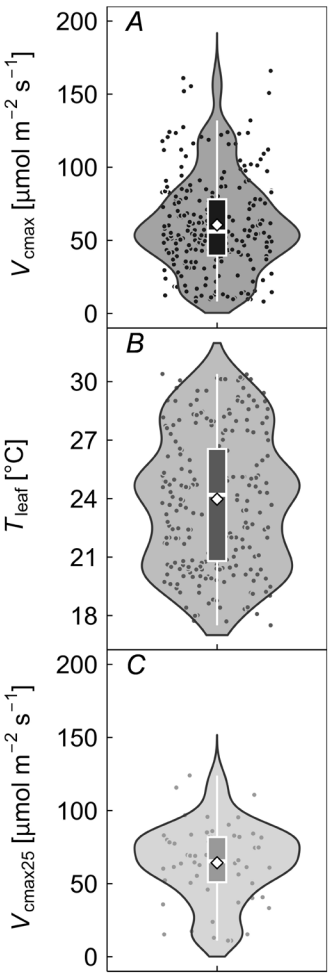

Fig. 2. Density plot, box plot, and scatter plot of the measured maximum carboxylation rate (V_{cmax}; *A*), leaf temperature (T_{leaf}; *B*), and V_{cmax} normalized to 25°C (V_{cmax25}; *C*). *The diamond* in each panel represents the mean value of each trait.

dataset was randomly divided into a sub-calibration dataset (80%) and a sub-validation dataset (20%) to select the optimal number of latent variables, which summarize the relationships between explanatory variables and objective variables. For each of the number of latent variables from 1 to 20, we constructed a PLSR model by cross-validation on the sub-calibration dataset and each PLSR model was applied to the sub-validation dataset to calculate the root mean square error of prediction, RMSEP. The optimal number of latent variables was determined as the smallest number whose RMSEP was within one standard error of the minimum RMSEP, based on PLSR models constructed with varying numbers of latent variables and applied to the sub-validation dataset. Then, a PLSR model was constructed by leave-one-out cross-validation on the calibration dataset for the optimal number of latent variables, and the PLSR model was applied to a validation dataset.

The prediction performance of the PLSR models was evaluated using the coefficient of determination (R^2), %RMSEP (RMSEP as a percentage of the trait range), and

BIAS (the difference between the mean predicted values and the mean observed values divided by the mean observed values). Moreover, to investigate which wavelengths were correlated with and contributed to the prediction of each leaf trait, we calculated regression coefficients and variable importance in projection (VIP) scores for each wavelength in the 450–850 nm range. VIP is a measure of the importance of an explanatory variable for predicting an objective variable. A VIP value greater than 1 indicates a strong contribution to the prediction using PLSR models (Chong and Jun 2005). Finally, to examine the factors contributing to V_{cmax} prediction, we calculated the score values, loading values, and contribution ratios of the first and second components (*i.e.*, latent variables) in PLSR model predicting V_{cmax}. Following that, we compared the relationships between the score values of the first and second components, and leaf temperature and V_{cmax25}. We conducted all statistical analyses in *R version 4.4.1* (R Core Team 2024) and used the '*spectratrait*' package (Burnett *et al*. 2021) for PLSR modeling.

Results

Measured leaf reflectance, leaf temperature, and photosynthetic traits: Leaf spectral reflectance showed a previously reported general pattern (Blackburn 2007; Fig. 3*A*). A small peak in the region of 500–600 nm was associated with the selective absorption of blue (around 460 nm) and red (around 630 nm) wavelengths by chlorophyll, which led to a relatively higher reflectance in the green wavelength range (around 550 nm) (Blackburn 2007). A sharp increase in reflectance was observed at the red edge (around 700 nm), followed by high reflectance in the near-infrared region (700–850 nm) (Blackburn 2007). The variation in leaf spectral reflectance with leaf temperature did not show a clear tendency. Specifically, reflectance in 450–750 nm exhibited little correlation with leaf temperature (*Pearson*'s correlation coefficient ranging from –0.05 to 0.1; Fig. 3*B*), while reflectance in 750–850 nm was weakly correlated with leaf temperature (*Pearson*'s correlation coefficient ranging from 0.1 to 0.25; Fig. 3*B*, *dashed line*). In addition, reflectance in 450–850 nm was moderately correlated with both V_{cmax} and V_{cmax25} (*Pearson*'s correlation coefficient ranging from –0.8 to –0.05; Fig. 3*B*, *solid and dotted-dashed lines*), though the correlation coefficient values were generally greater for V_{cmax} than for V_{cmax25} across 450–850 nm.

One criterion for assessing the accuracy of leaf spectral reflectance measurements is that the reflectance in 750–850 nm should fall in the range between 0.35 and 0.80 (Burnett *et al*. 2021). Although leaf reflectance values from 750–850 nm were relatively low, likely due to a larger port fraction (*i.e.*, the ratio of the opening area to the internal surface area) than the standard value of 0.05 (Fig. 4S), all spectral data measured in this study met this criterion, thereby confirming the reliability of the spectral measurements.

As noted in the materials and methods section, V_{cmax} was right-skewed (Fig. 2*A*). V_{cmax} values ranged from 8.16 to 165.95 µmol m^{-2} s^{-1}, with a mean value of 60.56 µmol m^{-2} s^{-1} and a median value of 55.96 µmol m^{-2} s^{-1}. The distribution of leaf temperature (T_{leaf}) values was not normal, but nearly symmetric (Fig. 2*B*). T_{leaf} values ranged from 17.5 to 30.4°C with a mean value of 24.0°C and a median value of 24.2°C. V_{cmax25} was normally distributed (Fig. 2*C*), and its values ranged from 11.00 to 124.00 µmol m^{-2} s^{-1} with a mean value of 64.28 µmol m^{-2} s^{-1} and a median value of 65.28 µmol m^{-2} s^{-1}.

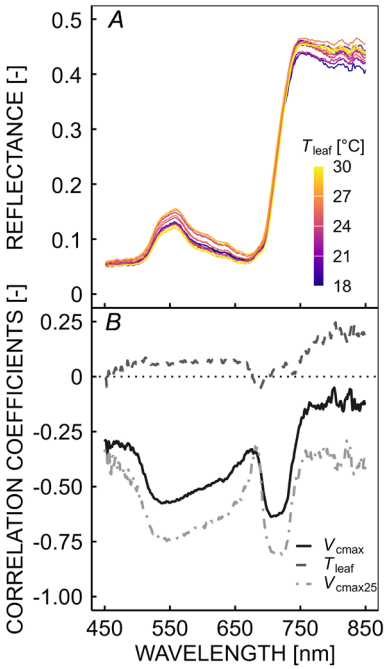

Fig. 3. Variation in leaf spectral reflectance in 450–850 nm with leaf temperature variation (*A*) and the *Pearson* correlation coefficient between each spectral reflectance in 450–850 nm and maximum carboxylation rate (V_{cmax}; *solid line*), leaf temperature (T_{leaf}; *dashed line*), and V_{cmax} normalized to 25°C (V_{cmax25}; *dotted-dashed line*) (*B*). *The color scale* in panel (*A*) represents the values of T_{leaf}. *The dotted line* in panel (*B*) represents a *Pearson* correlation coefficient of zero.

Prediction of leaf temperature and photosynthetic capacity from leaf reflectance: When leaf spectral reflectance from 450–850 nm was used as the explanatory variables, V_{cmax} and V_{cmax25} were moderately predicted (V_{cmax}: R^2 = 0.73, %RMSEP = 11.57%; V_{cmax25}: R^2 = 0.70, %RMSEP = 14.75%; Fig. 4*A*,*C*), though T_{leaf} was poorly predicted (R^2 = 0.32, %RMSEP = 21.44%; Fig. 4*B*). The BIAS of each PLSR model appeared to be close to zero (V_{cmax}: 0.022; T_{leaf}: 0.006; V_{cmax25}: –0.017). Using spectral reflectance from 450–700 nm as the explanatory variables reduced the prediction accuracy of each leaf trait compared with models using the 450–850 nm spectral range (V_{cmax}: R^2 = 0.59, %RMSEP = 14.36; T_{leaf}: R^2 = 0.17, %RMSEP = 23.66%; V_{cmax25}: R^2 = 0.57, %RMSEP = 17.71%; Fig. 5S, *supplement*).

In the PLSR model predicting V_{cmax}, the regression coefficient values ranged approximately from –15 to 15, showing a negative peak around 700 nm (Fig. 5*A*). VIP values exceeded 1 primarily in 530–590, 680–780,

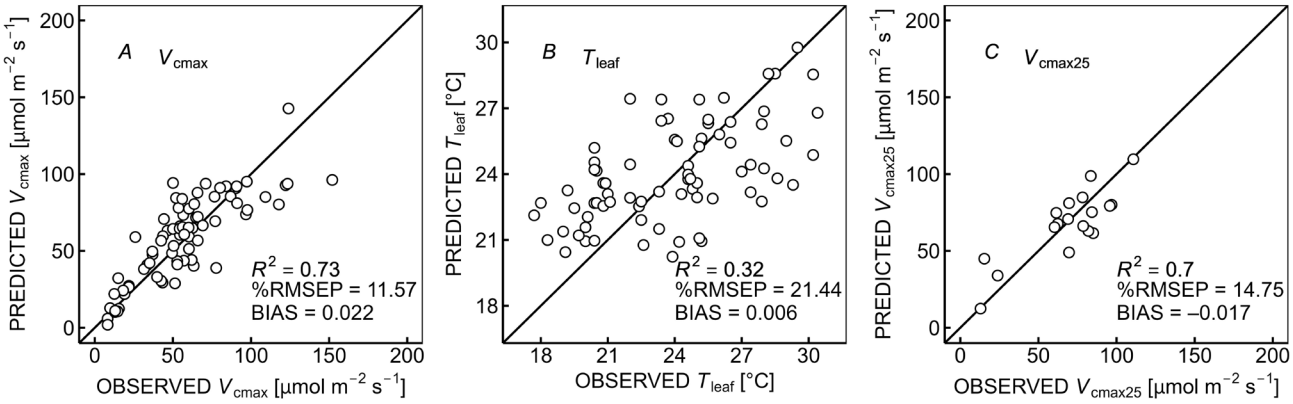

Fig. 4. Observed *vs.* predicted values of maximum carboxylation rate (V_{cmax}; *A*), leaf temperature (T_{leaf}; *B*), and V_{cmax} normalized to 25°C (V_{cmax25}; *C*) from partial least squares regression (PLSR) models using leaf spectral reflectance across 450–850 nm as explanatory variables. *The dashed lines* represent the 1:1 line.

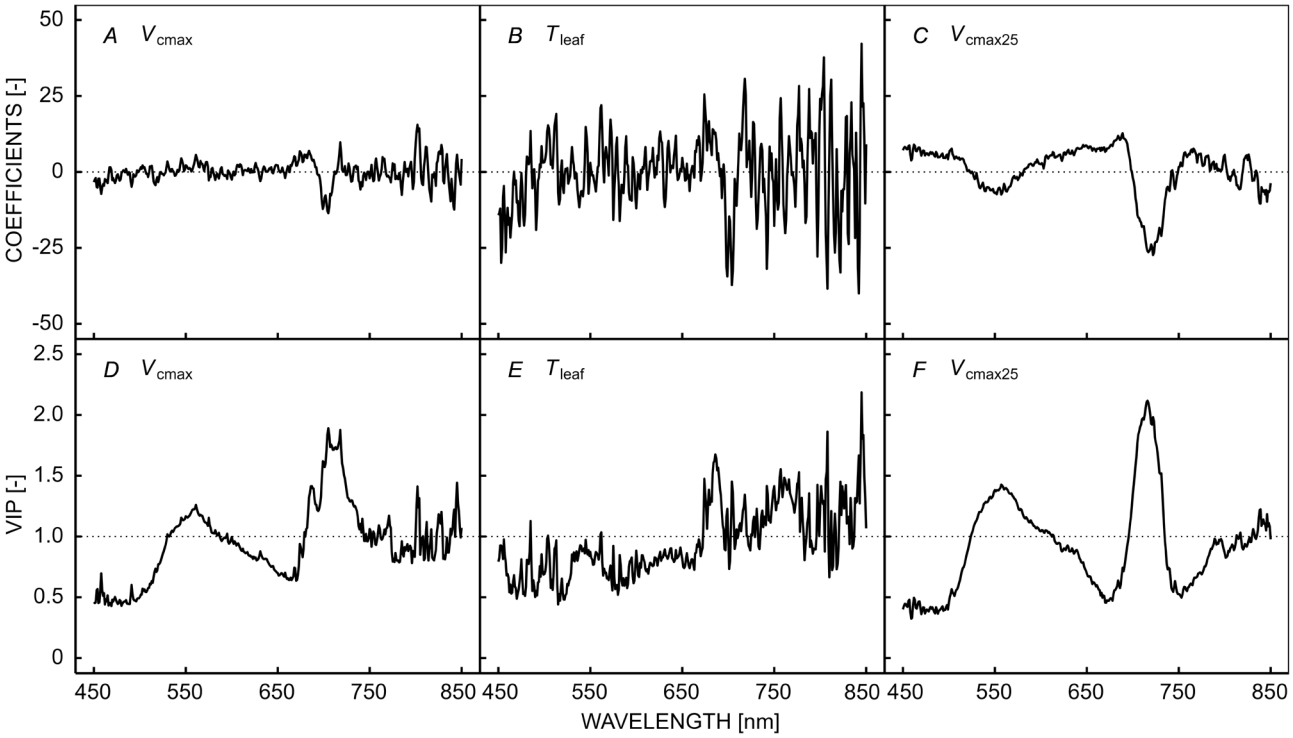

Fig. 5. Regression coefficient (*A–C*) and variable importance in projection, VIP (*D–F*) values from partial least squares regression, PLSR models predicting maximum carboxylation rate (V_{cmax}; *A*,*D*), leaf temperature (T_{leaf}; *B*,*E*), and V_{cmax} normalized to 25°C (V_{cmax25}; *C*,*F*). *The dotted lines* in panel (*A–C*) represent a coefficient value of zero, while *the dotted lines* in panel (*D–F*) represent a VIP value of one.

and 800–850 nm (Fig. 5*D*). In the prediction of T_{leaf}, the regression coefficient values ranged approximately from –50 to 50, with a negative peak around 700 nm and alternating increases and decreases (Fig. 5*B*), and VIP values exceeded 1 mainly in 670–850 nm (Fig. 5*E*). In the prediction of V_{cmax25}, the regression coefficient values ranged from –30 to 15, with negative peaks at 550 and 720 nm (Fig. 5*C*), and VIP values exceeded 1 primarily in 520–615, 695–735, and 815–850 nm (Fig. 5*F*).

In the PLSR model predicting V_{cmax} from leaf spectral reflectance across 450–850 nm, the number of components (*i.e.*, latent variables) was six. The first and second components respectively explained 75.4 and 15.2% of the variation in V_{cmax} within the calibration dataset (Fig. 6*A*). The score values of the first component appeared to vary with V_{cmax25} (Fig. 6*A*) and indeed, they were moderately correlated with V_{cmax25} (r = 0.72, p<0.001; Fig. 6*C*). Meanwhile, the score values of the second component were weakly correlated with T_{leaf} (r = 0.24, p = 0.001; Fig. 6*D*). The loading values of the first component showed negative peaks around 550 and 720 nm, while those of the second component showed negative peaks at similar wavelengths and a positive plateau across 750–850 nm (Fig. 6*B*). Moreover, in the PLSR model predicting V_{cmax}

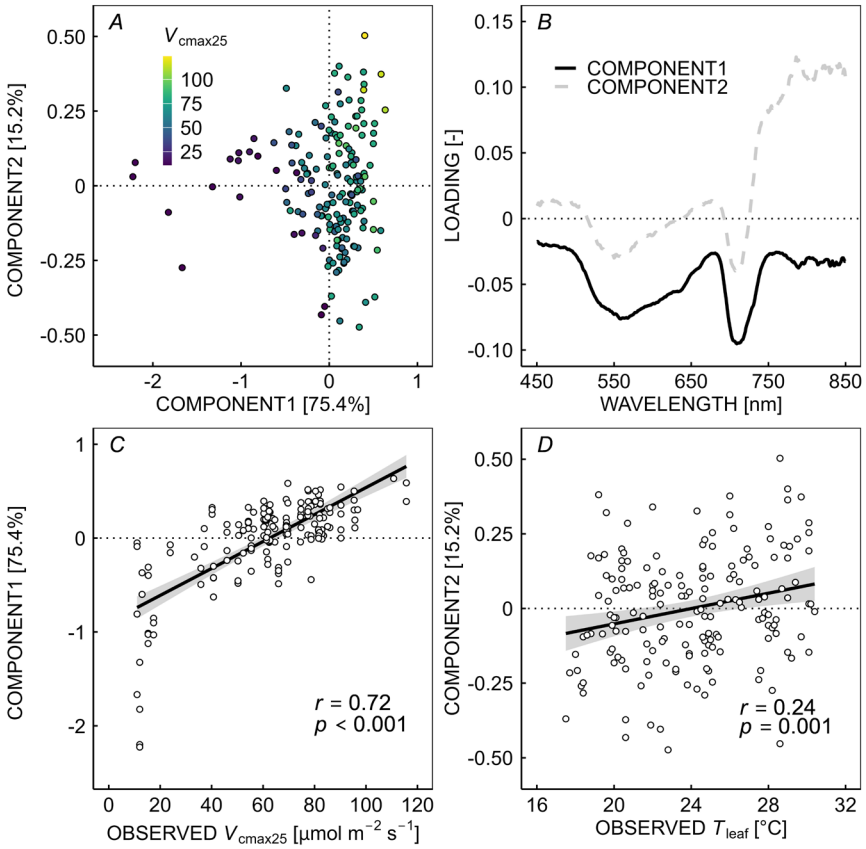

Fig. 6. Relationships between the first and second components of the partial least squares regression (PLSR) model for maximum carboxylation rate (V_{cmax}): relationships between the score values of the first and second components (*A*), the loading values of the first and second components (*B*), observed V_{cmax} normalized to 25°C (V_{cmax25}) and the score values of the first component (*C*), and leaf temperature (T_{leaf}) and the score values of the second component (*D*). In each panel, *the dotted lines* indicate a score or loading value of zero. *The color scale* in panel (*A*) indicates observed V_{cmax25} in the calibration dataset. *The black solid* and *the gray dashed lines* in panel (*B*) represent the loadings of the first and second components, respectively. In panels (*C*) and (*D*), *the solid lines* indicate linear regression fits, and *the shaded areas* represent the 95% confidence intervals.

from leaf spectral reflectance across 450–700 nm, the first component explained 94.4% of the variation in V_{cmax} and its score values were also correlated with V_{cmax25} ($r = 0.68$, $p<0.001$; Fig. 6S, *supplement*).

Discussion

In this study, to explore the underlying mechanism of V_{cmax} prediction from spectral reflectance in 450–850 nm, we predicted leaf temperature and V_{cmax25} in addition to V_{cmax} and evaluated the influence of leaf temperature or V_{cmax25} on the prediction of V_{cmax}. V_{cmax} was predicted with moderate accuracy from spectral reflectance not only in 450–850 nm ($R^2 = 0.73$, %RMSEP = 11.57%; Fig. 4*A*) but also in 450–700 nm ($R^2 = 0.59$, %RMSEP = 14.36%; Fig. 5S*A*). These prediction accuracies were consistent with those reported in previous studies using leaf spectral reflectance within 450–850 nm as predictors (Silva-Perez *et al.* 2018: $R^2 = 0.57$, Fu *et al.* 2020: $R^2 = 0.78$, Meacham-Hensold *et al.* 2020: $R^2 = 0.67$, Sexton *et al.* 2021: $R^2 = 0.55$, Buchaillot *et al.* 2022: $R^2 = 0.63$). In addition, the accuracy obtained in this study was comparable to that reported in previous studies using not only linear approaches, such as PLSR, but also non-linear approaches, including artificial neural networks and support vector machines (Fu *et al.* 2019, Kumagai *et al.* 2022). This suggests that the choice of PLSR as the modeling approach in this study is unlikely to have affected the prediction accuracy.

While V_{cmax} was moderately predicted, the leaf temperature prediction accuracies using the spectral reflectance in both 450–850 nm and 450–700 nm were low ($R^2 = 0.32$, Fig. 4*B*; $R^2 = 0.17$, Fig. 5S*B*). These results suggest that leaf spectral reflectance ranging from 450–850 nm, particularly 700–850 nm, partially captures variations in leaf temperature. Moreover, leaf temperature was more strongly correlated with reflectance in 700–850 nm than with reflectance in 450–700 nm (Fig. 3*B*), supporting the idea that reflectance in 700–850 nm contributes to the prediction of leaf temperature. These findings were consistent with previous studies that predicted leaf temperature using wavelengths across the VIS–NIR–SWIR range (400–2,500 nm), in which leaf temperature was primarily predicted using wavelengths in the NIR and SWIR regions (700–2,500 nm; Khan *et al.* 2021). One possible explanation for why leaf temperature is predicted using wavelengths in the NIR–SWIR region rather than the VIS region (400–700 nm) lies in

the differences in light absorption processes between these spectral regions. In the VIS region, light absorption occurs through electronic transitions, which are relatively insensitive to temperature changes, whereas in the NIR–SWIR region, absorption is primarily due to molecular vibrations, which are more sensitive to temperature (Cozzolino *et al*. 2007). For instance, it has been reported that water, which is abundant in leaves, has absorption bands in the NIR–SWIR region (*e.g*., 1,450; 1,940 nm), and the peak wavelengths of these bands shift in proportion to temperature (Czarnik-Matusewicz *and* Pilorz 2006). Indeed, it is known that the temperature of water can be predicted based on changes in the absorptance of water associated with temperature variations (Kakuta *et al*. 2011).

Despite the poor prediction accuracy of leaf temperature, the prediction accuracy of V_{cmax25} was comparable to that of the V_{cmax} (V_{cmax25}: R^2 = 0.70, %RMSEP = 14.75%; V_{cmax}: R^2 = 0.73, %RMSEP = 11.57%; Fig. 4*A*,*C*), and the peak VIP values were mostly matched at around 550 and 720 nm (Fig. 5*D*,*F*). In particular, the peaks of VIP at around 550 and 720 nm in both V_{cmax25} and V_{cmax} predictions were consistent with the pattern of the *Pearson*'s correlation coefficient values between the spectral reflectance around these wavelengths (550 and 720 nm) and V_{cmax25} (Fig. 3*B*). Our VIP analysis was also consistent with previous studies (Yendrek *et al*. 2017, Wang *et al*. 2021, Yan *et al*. 2021), which attributed these features primarily to chlorophyll absorption (Yendrek *et al*. 2017, Wang *et al*. 2021, Yan *et al*. 2021). Therefore, the prediction of V_{cmax} from spectral reflectance in 450–850 nm appears to be largely based on the variation of V_{cmax25} explained by chlorophyll absorption. Regarding the first component of the PLSR model predicting V_{cmax}, the score values varied largely with V_{cmax25}, and the variation and peak pattern of loading values closely matched those of the *Pearson*'s correlation coefficients between the spectral reflectance and V_{cmax25}, as well as the regression coefficients and VIP values for V_{cmax25} prediction (Fig. 3*B*; Fig. 6*A*,*C*). These findings suggest that the first component of the PLSR model predicting V_{cmax} would represent the variation of V_{cmax25}. Given that the first component explains 75.4% of the variation in V_{cmax} in the PLSR model using leaf spectral reflectance across 450–850 nm and 94.4% of V_{cmax} variation in the model using leaf spectral reflectance across 450–700 nm, the variation in V_{cmax25} would determine the variation in predicted V_{cmax} derived from spectral reflectance in 450–700 nm.

However, these findings also imply that 24.6% of the predicted variation in V_{cmax} from leaf spectral reflectance across 450–850 nm is determined by factors other than V_{cmax25}. In fact, the score of the second component in the V_{cmax} prediction was weakly correlated with leaf temperature (Fig. 6*D*). This relationship was further supported by the similarity between the loading pattern of the second component in V_{cmax} prediction and the correlation coefficients linking leaf temperature to individual spectral reflectance values within 450–850 nm (Fig. 3*B*, Fig. 6*B*). Moreover, the *Pearson*'s correlation coefficients for V_{cmax} within 750–850 nm appeared to reflect the offset between the correlation coefficients for leaf temperature and V_{cmax25} because the correlation coefficients for leaf temperature in this region were positive, while those for V_{cmax25} were strongly negative. Therefore, the second component of the PLSR model predicting V_{cmax} from the spectral reflectance across 450–850 nm may partially reflect variations in leaf temperature, especially suggesting that reflectance within 700–850 nm partly captures temperature-induced variations in V_{cmax}. Furthermore, this finding implies that it cannot be stated that the temperature-dependent parameters of V_{cmax} can be captured by spectral reflectance in 450–850 nm. For instance, Serbin *et al*. (2015) reported that activation energy (*i.e.*, E_a) of V_{cmax} can be predicted from spectral reflectance in 400–2,500 nm using a PLSR model. Although it is difficult to discuss the influence of E_a in V_{cmax} prediction based on the results obtained in this study, future research may provide insight into the prediction mechanism of temperature response of V_{cmax} from spectral reflectance in 450–850 nm by predicting E_a in addition to V_{cmax}.

Conclusion: To provide preliminary insights into how leaf spectral reflectance in 450–850 nm predicts the temperature-driven variation in V_{cmax}, we predicted V_{cmax}, leaf temperature, and V_{cmax25} using PLSR models. Using the spectral reflectance in 450–850 nm, V_{cmax} and V_{cmax25} were moderately predicted (R^2 = 0.73 and 0.70, respectively), while leaf temperature was weakly predicted (R^2 = 0.32). Meanwhile, using the spectral reflectance in 450–700 nm, the prediction accuracy of each leaf trait declined (R^2 = 0.59 for V_{cmax} and 0.57 for V_{cmax25}), especially for leaf temperature (R^2 = 0.17). Additionally, to assess the influence of leaf temperature and V_{cmax25} on the prediction of V_{cmax}, we compared the relationships between these variables and the score values of the first and second components in the PLSR model for V_{cmax}. The score values of the first component in the PLSR model for V_{cmax} using reflectance in 450–850 nm explained 75.4% of the variation in V_{cmax}, and the model using reflectance in 450–700 nm explained 94.4% of that, and both first components were correlated with V_{cmax25} (r = 0.72 and 0.67, respectively). In contrast, in the model using reflectance in 450–850 nm, the score values of the second component explained 15.2% of the variation in V_{cmax} and were weakly correlated with leaf temperature (r = 0.24). These findings suggest that V_{cmax} prediction from spectral reflectance in 450–700 nm is primarily driven by V_{cmax25}, while spectral reflectance in 700–850 nm partially contributes to capturing leaf temperature, and possibly temperature-induced variations in V_{cmax}.

References

Bernacchi C.J., Bagley J.E., Serbin S.P. *et al*.: Modeling C_3 photosynthesis from the chloroplast to the ecosystem. – Plant Cell Environ. **36**: 1641-1657, 2013.

Bernacchi C.J., Singsaas E.L., Pimentel C. *et al*.: Improved temperature response functions for models of Rubisco-limited photosynthesis. – Plant Cell Environ. **24**: 253-259, 2001.

Blackburn G.A.: Hyperspectral remote sensing of plant pigments. – J. Exp. Bot. **58**: 855-867, 2007.

Buchaillot M.L., Soba D., Shu T. *et al*.: Estimating peanut and

soybean photosynthetic traits using leaf spectral reflectance and advanced regression models. – Planta **255**: 93, 2022.

Burnett A.C., Anderson J., Davidson K.J. *et al.*: A best practice guide to predicting plant traits from leaf-level hyperspectral data using partial least squares regression. – J. Exp. Bot. **72**: 6175-6189, 2021.

Burnett A.C., Davidson K.J., Serbin S.P., Rogers A.: The "one-point method" for estimating maximum carboxylation capacity of photosynthesis: A cautionary tale. – Plant Cell Environ. **42**: 2472-2481, 2019.

Chong I.-G., Jun C.-H.: Performance of some variable selection methods when multicollinearity is present. – Chemom. Intell. Lab. Syst. **78**: 103-112, 2005.

Cozzolino D., Liu L., Cynkar W.U. *et al.*: Effect of temperature variation on the visible and near infrared spectra of wine and the consequences on the partial least square calibrations developed to measure chemical composition. – Anal. Chim. Acta **588**: 224-230, 2007.

Croft H., Chen J.M., Luo X. *et al.*: Leaf chlorophyll content as a proxy for leaf photosynthetic capacity. – Glob. Change Biol. **23**: 3513-3524, 2017.

Czarnik-Matusewicz B., Pilorz S.: Study of the temperature-dependent near-infrared spectra of water by two-dimensional correlation spectroscopy and principal components analysis. – Vib. Spectrosc. **40**: 235-245, 2006.

De Kauwe M.G., Lin Y.-S., Wright I.J. *et al.*: A test of the 'one-point method' for estimating maximum carboxylation capacity from field-measured, light-saturated photosynthesis. – New Phytol. **210**: 1130-1144, 2016.

Dechant B., Cuntz M., Vohland M. *et al.*: Estimation of photosynthesis traits from leaf reflectance spectra: Correlation to nitrogen content as the dominant mechanism. – Remote Sens. Environ. **196**: 279-292, 2017.

Duursma R.A.: Plantecophys – an R package for analysing and modelling leaf gas exchange data. – PLoS ONE **10**: e0143346, 2015.

Farquhar G.D., von Caemmerer S., Berry J.A.: A biochemical model of photosynthetic CO_2 assimilation in leaves of C_3 species. – Planta **149**: 78-90, 1980.

Fu P., Meacham-Hensold K., Guan K., Bernacchi C.J.: Hyperspectral leaf reflectance as proxy for photosynthetic capacities: an ensemble approach based on multiple machine learning algorithms. – Front. Plant Sci. **10**: 730, 2019.

Fu P., Meacham-Hensold K., Guan K. *et al.*: Estimating photosynthetic traits from reflectance spectra: A synthesis of spectral indices, numerical inversion, and partial least square regression. – Plant Cell Environ. **43**: 1241-1258, 2020.

Hikosaka K., Ishikawa K., Borjigidai A. *et al.*: Temperature acclimation of photosynthesis: mechanisms involved in the changes in temperature dependence of photosynthetic rate. – J. Exp. Bot. **57**: 291-302, 2006.

Kakuta N., Fukuhara Y., Kondo K. *et al.*: Temperature imaging of water in a microchannel using thermal sensitivity of near-infrared absorption. – Lab Chip **11**: 3479-3486, 2011.

Kattge J., Knorr W., Raddatz T., Wirth C.: Quantifying photosynthetic capacity and its relationship to leaf nitrogen content for global-scale terrestrial biosphere models. – Glob. Change Biol. **15**: 976-991, 2009.

Khan H.A., Nakamura Y., Furbank R.T., Evans J.R.: Effect of leaf temperature on the estimation of photosynthetic and other traits of wheat leaves from hyperspectral reflectance. – J. Exp. Bot. **72**: 1271-1281, 2021.

Knipling E.B.: Physical and physiological basis for the reflectance of visible and near-infrared radiation from vegetation. – Remote Sens. Environ. **1**: 155-159, 1970.

Kubota S., Yokoyama G., Shibata T. *et al.*: Stomatal, mesophyll, and biochemical limitation to photosynthesis of soybeans under waterlogging and reoxygenation. – Environ. Exp. Bot. **243**: 106325, 2026.

Kumagai E., Burroughs C.H., Pederson T.L. *et al.*: Predicting biochemical acclimation of leaf photosynthesis in soybean under in-field canopy warming using hyperspectral reflectance. – Plant Cell Environ. **45**: 80-94, 2022.

Meacham-Hensold K., Fu P., Wu J. *et al.*: Plot-level rapid screening for photosynthetic parameters using proximal hyperspectral imaging. – J. Exp. Bot. **71**: 2312-2328, 2020.

Nakai H., Yasutake D., Hidaka K. *et al.*: Starch serves as an overflow product in the regulation of carbon allocation in strawberry leaves in response to photosynthetic activity. – Plant Growth Regul. **101**: 875-882, 2023.

R Core Team: *R*: A language and environment for statistical computing. R Foundation for Statistical Computing, Vienna, 2024. *Available at*: https://www.R-project.org/.

Sawatsky M.L., Clyde M., Meek F.: Partial least squares regression in the social sciences. – Quant. Meth. Psych. **11**: 52-62, 2015.

Serbin S.P., Dillaway D.N., Kruger E.L. *et al.*: Leaf optical properties reflect variation in photosynthetic metabolism and its sensitivity to temperature. – J. Exp. Bot. **63**: 489-502, 2012.

Serbin S.P., Singh A., Desai A.R. *et al.*: Remotely estimating photosynthetic capacity, and its response to temperature, in vegetation canopies using imaging spectroscopy. – Remote Sens. Environ. **167**: 78-87, 2015.

Sexton T., Sankaran S., Cousins A.B.: Predicting photosynthetic capacity in tobacco using shortwave infrared spectral reflectance. – J. Exp. Bot. **72**: 4373-4383, 2021.

Silva-Perez V., Molero G., Serbin S.P. *et al.*: Hyperspectral reflectance as a tool to measure biochemical and physiological traits in wheat. – J. Exp. Bot. **69**: 483-496, 2018.

Wang S., Guan K., Wang Z. *et al.*: Unique contributions of chlorophyll and nitrogen to predict crop photosynthetic capacity from leaf spectroscopy. – J. Exp. Bot. **72**: 341-354, 2021.

Wilson K.B., Baldocchi D.D., Hanson P.J.: Spatial and seasonal variability of photosynthetic parameters and their relationship to leaf nitrogen in a deciduous forest. – Tree Physiol. **20**: 565-578, 2000.

Wold S., Sjöström M., Eriksson L.: PLS-regression: a basic tool of chemometrics. – Chemom. Intell. Lab. Syst. **58**: 109-130, 2001.

Yan Z., Guo Z., Serbin S.P. *et al.*: Spectroscopy outperforms leaf trait relationships for predicting photosynthetic capacity across different forest types. – New Phytol. **232**: 134-147, 2021.

Yendrek C.R., Tomaz T., Montes C.M. *et al.*: High-throughput phenotyping of maize leaf physiological and biochemical traits using hyperspectral reflectance. – Plant Physiol. **173**: 614-626, 2017.